

Learning-based Handover in Mobile Millimeter-wave Networks

Sara Khosravi, *Student Member, IEEE*, Hossein S. Ghadikolaei, *Member, IEEE*, and Marina Petrova, *Member, IEEE*

Abstract—Millimeter-wave (mmWave) communication is considered as a key enabler of ultra-high data rates in the future cellular and wireless networks. The need for directional communication between base stations (BSs) and users in mmWave systems, that is achieved through beamforming, increases the complexity of the channel estimation. Moreover, in order to provide better coverage, dense deployment of BSs is required which causes frequent handovers and increased association overhead. In this paper, we present an approach that jointly addresses the beamforming and handover problems. Our solution entails an efficient beamforming method with a few number of pilots and a learning-based handover method supporting mobile scenarios. We use reinforcement learning algorithm to learn the optimal choices of the backup BSs in different locations of a mobile user. We show that our method provides an almost constant rate and reliability in all locations of the user’s trajectory with a small number of handovers. Simulation results in an outdoor environment based on narrow band cluster mmWave channel modeling and real building map data show the superior performance of our proposed solution in achievable instantaneous rate and trajectory rate.

Index Terms—Wireless communications, millimeter-wave networks, beamforming, handover, reinforcement learning.

I. INTRODUCTION

THE expected growth of the mobile traffic and high data rate demands has triggered the design of communication systems that operate in millimeter-wave (mmWave) bands [1]. The main advantage of moving to the mmWave spectrum is the availability of huge bandwidth in comparison to the conventional sub-6 GHz spectrum. However, mmWave bands are severely affected by obstacles unlike the sub-6 GHz bands for two main reasons. First, due to an order of magnitude smaller wavelength, the signals cannot diffract well against most common materials in urban environments, leading to severe penetration loss and blockage [1]. Second, the need for using directional communication to compensate for the high propagation loss, increases the beam misalignment chance, especially in the presence of many obstacles when there is a need to frequently update the beamforming vectors [2]–[4]. Establishing and maintaining mmWave links are even more challenging in mobile environments where both the users and obstacles are moving. In order to provide good coverage and improve the capacity, base station (BS) densities need to be significantly higher in mmWave network [5], [6]. These bring new challenges when compared to the sub-6 GHz networks

[7]. For example, providing a reliable connection through UE’s trajectory while balancing the number of handovers is a key design challenge to be solved if the mmWave networks are to support Gbps data rate for mobile users. In order to address this challenge, an efficient beamforming method is required to enable low latency and signaling overhead. In this paper, we jointly address the handover and beamforming challenges. In the next subsection, we describe our main contributions.

A. Our Contributions

The main objective of this paper is to develop an efficient and lightweight joint handover and beamforming method that maintains a predefined level of throughput along the UE’s trajectory. More specifically, we address the following questions.

- How can sparsity and correlation of valid paths between the BS and the user equipment (UE) be used to design an efficient beamforming? We propose a beamforming algorithm based on constructing and maintaining a database of path skeletons, i.e., available paths between the BS and the UE. In our proposed algorithm, beam searching will only run through the path skeletons not through all the directions. Moreover, our algorithm tracks the correlation between path skeletons in different locations of the UE and queries a new path skeleton only when a significant change such as a sudden blockage has occurred.
- How can a handover method be designed to provide a reliable connection in mobile scenarios? We propose a learning-based handover method based on keeping an updated backup channel for the serving BS. We use reinforcement learning (RL) to optimize the list of the backup BSs. Our method comprises two decision making phases. In the first phase, our algorithm makes a decision regarding pinging a good backup BS. We model this selection process as an RL problem that takes the mobility prediction information as input and returns the best candidate BSs as the backup for a specific location. In the second decision making phase, our algorithm uses the channel estimation results of the both serving and backup BSs and makes the handover execution decision.
- *What are the benefits of our proposed method?* We compare our proposed approach with two relevant baselines in the literature. We numerically compare the key performance indicators including number of handovers, connection reliability, instantaneous rate and trajectory rate of our approach with the baselines. The results indicate that our proposed approach substantially outperforms the baselines in terms of number of handovers

S. Khosravi, H. S. Ghadikolaei and M. Petrova are with school of EECS, KTH Royal Institute of Technology, Stockholm, Sweden (emails: {sarakhos, hshokri, petrovam}@kth.se). The work of H. S. Ghadikolaei was partially supported by the Swedish Research Foundation under grant 2018-00820.

and more importantly connection reliability throughout the trajectory.

- *What is the performance of our proposed method in a realistic channel model?* We use ray tracing with real building data map as the input. We also add common blockages like human bodies and cars to the simulation area in order to evaluate the performance of our method in a more realistic environment.

We conclude that our solution is a signaling-efficient and lightweight approach that properly design the beamforming and handover so as to maintain a predefined quality-of-service level for the mmWave users in a dynamic and non-stationary environment. In the following, we will review state-of-the-art approaches for beamforming and handover in mmWave networks.

B. Related work

Most of the mmWave beamforming approaches are carried out the exhaustive beam-searching over a set of pre-defined beams to find the beam pairs between a BS and a UE with the optimal alignment [8], [9]. However, due to the high dimension of the beam-searching, these approaches increase the overhead significantly. Even other approaches, such as sparsity-aware beamforming [10] or subspace estimation [11] suffer from the overhead in mobile scenarios. The recent compressive-sensing based approaches [10], [12], [13] need logarithmic number of the measurements during the beam-searching phase. However, due to the need of an adopted phase-array antennas [13] or phase coherent measurements [12], they may not work well with existing mmWave devices.

The authors in [14], [15] presented the beam-searching methods which used the sparsity and the correlation of spatial channel response of mmWave channels in adjacent locations. Despite of their promising results in terms of throughput, those methods are validated on stationary users [14] or increase the complexity of the beam-searching phase [15] thereby, constraining their applicability in real mobile scenarios. However, in this work, inspired by the idea of path skeleton in [14], we propose an efficient approach to maintain the path-skeleton and track the correlation of path skeletons during the beam-searching phase. The overhead of our approach reduces as the number of UEs grows large, making it very useful for massive wireless access scenarios.

When it comes to the design of efficient and robust handover algorithms, the related state of the works can be grouped in three categories: learning-based handover [16]–[22], side information [21]–[25], and multi-connectivity [26]–[29].

To make the optimal handover decision, leveraging machine learning as the main decision maker tool can be an effective approach. In [16], authors used Markov decision process (MDP) in order to maximize the throughput and the achieved rate. However, due to the computation complexity of solving MDP, it cannot be directly applied to dense networks. The authors in [17] proposed a novel handover policy based on the RL framework for the radio access network slicing. References [18] and [19] proposed a learning algorithm to manage vertical handovers in heterogeneous networks. The authors in [20]

introduced an RL-based handover policy named *SMART* to reduce the number of the handovers while keeping the UE's quality-of-service in the heterogeneous network. However, the aim of our proposed algorithm is to maximize the long-term rewards (trajectory rate) and provide a reliable connection which is a function of both handover and beamforming in every slot. To this end, we propose an efficient beamforming method with low signaling overhead and propose a handover algorithm which maximizes the long-term reward by using statistical information of the mobility class and blockage distribution. Our approach, despite most of the the existing handover methods based on instantaneous change gain, prevent the ping-pong effect and lower trajectory rate due to the long-term view. Based on the simulation results, our approach outperforms *SMART* method in terms of the connection reliability and the number of the handovers.

The authors in [21], [22] used the camera information to estimate the location of different obstacles and presented a proactive learning-based handover policy. However, due to the high density and variety of the obstacles in the urban environment, estimating the location of all obstacles may increase the network overhead. Our proposed learning-based handover method does not need online tracking of the obstacles and with keeping the connection toward a backup BS makes the handover decision.

Side information or context-aware aided approaches make use of the location of the user or the obstacles in order to make a handover decision. The work in [23] showed the importance of the location information in scaling mmWave networks to the dense and dynamic environment. Authors in [24] proposed a handover method which leverages channel measurement of dominant line-of-sight (LoS) path of serving BSs in order to estimate the LoS path properties of other BSs toward the UE and then ranks BSs based on predicted beam strength. However, this method may not be applicable in all scenarios because this method cannot estimate good non-LoS (NLoS) paths in a crowded environment. However, our proposed approach considers all available paths in the path skeleton set of serving BS and backup BS toward the UE during the channel estimation phase and use the RL in order to select the backup channel.

In the multi-connectivity methods, a UE maintains its connection to multiple BSs (either at the mmWave or sub-6 GHz bands). Simultaneous connection of a UE with multiple BSs is analyzed vastly in [26]–[29] as a solution to the link failure and the throughput degradation in a dynamic environment. However, power consumption, synchronization and the necessity of frequent tracking are main challenges of multi-connectivity methods. For example, although different multi-connectivity schemes proposed in [26] may improve the session-level mmWave operation in a realistic environment, the presented schemes need additional connection-probe procedures and knowledge of the mmWave system state which add the overhead to the network. Our proposed approach is based on keeping UE's connection toward a backup mmWave BS with low overhead during the channel estimation by sending pilot signals only through the path skeleton sets.

Table I: Nomenclatures.

Notation	Description
j, N	Index and total number of BSs in a zone
i, M	Location index and the length of a trajectory
p, P	Index and total number of path clusters in a PS set
ℓ, L	Index and total number of SNR levels
SNR	Signal to noise ratio
PS	Path skeleton set
\mathbf{f}, \mathbf{w}	Beamforming and combining vectors
σ^2	Thermal noise power
W	Signal bandwidth
\mathbf{H}	Channel matrix
$\mathbf{u}_{\text{BS}}(\cdot), \mathbf{u}_{\text{UE}}(\cdot)$	Array response of BS and UE antennas
$\theta^{\text{UE}}, \phi^{\text{UE}}$	Horizontal and vertical AoA
$\theta^{\text{BS}}, \phi^{\text{BS}}$	Horizontal and vertical AoD
$h_{r,p}$	channel gain of r -th subpath of path cluster p
$N_{\text{BS}}, N_{\text{UE}}$	Number of BS and UE antennas
Handover algorithm parameters	
$\text{BS}_S^k, \text{BS}_B^k$	Serving and backup BS in CI k
$\text{SNR}^\ell(\text{BS}_S^k, i)$	SNR level ℓ from BS_S^k toward UE in location i
t_{Log}	Age of the SNR in terms of CI
T_{HO}	Handover threshold
T_{D}	PS distance threshold
T_{Aging}	Aging threshold of a PS in the database

C. Organization and Notation

The rest of the paper is organized as follows. We introduce our system model in Section II. Then, we describe our beamforming method and handover algorithm in Section III. We model the problem of choosing backup BS as an RL problem in Section IV. We numerically evaluate our algorithm in Section V. Finally, we conclude our work in Section VI.

Notation: Matrices, vectors and scalars are denoted by bold upper-case (\mathbf{X}), bold lower-case (\mathbf{x}) and non-bold (x) letters, respectively. The ℓ_2 -norm, transpose, and conjugate transpose of a vector \mathbf{x} (or a matrix \mathbf{X}) are $\|\mathbf{x}\|$, \mathbf{x}^T , and \mathbf{x}^H , respectively. We define set $[M] = \{1, 2, \dots, M\}$ for any integer M .

II. SYSTEM MODEL

In this section, we introduce our main assumptions and system model. Table I summarizes our main notations.

We consider the downlink of a mmWave network with N BSs and mobile UEs. We assume a two-dimensional Poisson point process (PPP) with density ρ for the spatial distributions of the BSs, though our proposed algorithmic framework can work for any other model. We assume all BSs allocate equal resources to their serving UEs. Extension to the load balancing at the BS for multiple UEs scenario are left for the future work.

We employ a narrow band cluster 3D channel model [2] with small number of clusters and N_{BS} antennas at the BS and N_{UE} antennas at the UE side. In this model the channel matrix $\mathbf{H} \in \mathbb{C}^{N_{\text{BS}} \times N_{\text{UE}}}$ between a UE in location i of a trajectory (with M points) and BS_j , $j \in [N]$ is fixed during a coherence interval (CI) and can be defined as:

$$\mathbf{H}(j, i) = \frac{1}{\sqrt{R}} \sum_{p=1}^P \sum_{r=1}^R h_{r,p} \mathbf{u}_{\text{UE}}(\theta_{r,p}^{\text{UE}}, \phi_{r,p}^{\text{UE}}) \mathbf{u}_{\text{BS}}^H(\theta_{r,p}^{\text{BS}}, \phi_{r,p}^{\text{BS}}), \quad (1)$$

where P is the number of path clusters and R is the number of subpaths in each cluster. Each subpath has the horizontal and vertical angle of arrivals (AoAs), $\theta_{r,p}^{\text{UE}}, \phi_{r,p}^{\text{UE}}$, and horizontal and

vertical angle of departures (AoDs), $\theta_{r,p}^{\text{BS}}, \phi_{r,p}^{\text{BS}}$, respectively. $h_{r,p}$ is the complex gain of r -th subpath of cluster p which includes both the path loss and small scale fading [2]. We generate these parameters based on different distribution as given in [2, Table I]. For the sake of notation simplicity, we drop the notation i and j from the the channel parameters, whenever they are clear from the context. We consider a half wavelength uniform planar arrays of antennas both at the BS and the UE sides which can be defined as [30]:

$$\mathbf{u}_s(\theta^s, \phi^s) = [1, \dots, e^{j\pi[n_{\text{BS}} \sin(\theta) \cos(\phi) + n_{\text{UE}} \sin(\theta) \sin(\phi)]}, \dots]^T \quad (2)$$

where $1 \leq n_{\text{BS}} \leq N_{\text{BS}} - 1$, $1 \leq n_{\text{UE}} \leq N_{\text{UE}} - 1$, and $s \in \{\text{UE}, \text{BS}\}$.

We use the following probability functions obtained based on the New York City measurements in [31] to define the probability of LoS and NLoS states of each link:

$$p_{\text{LoS}}(d) = \left[\min\left(\frac{27}{d}, 1\right) \cdot \left(1 - e^{-\frac{d}{71}}\right) + e^{-\frac{d}{71}} \right]^2 \quad (3a)$$

$$p_{\text{NLoS}}(d) = 1 - p_{\text{LoS}}(d), \quad (3b)$$

where d is the 3D distance between UE and BS in meters. We model the pathloss of the LoS and NLoS links as:

$$\text{PL}(d)[\text{dB}] = 10 \log_{10} \left(\frac{4\pi d_0}{\lambda} \right)^2 + 10\hat{n} \log_{10} \left(\frac{d}{d_0} \right) + X_\mu, \quad (4)$$

where d_0 is the close-in free space reference distance which in this work $d_0 = 1$, λ is the wavelength, \hat{n} is the path loss exponent, and X_μ is a zero mean Gaussian random variable with the standard deviation μ in dB which represents the shadow fading. \hat{n} and μ have different amounts for LoS and NLoS links. These parameters are given in [32, Table V and VI].

The signal to noise ratio (SNR) at the UE in location i which is serving by BS_j can be defined as

$$\text{SNR}(j, i) = \frac{|\mathbf{w}^H(i) \mathbf{H}(j, i) \mathbf{f}(j, i)|^2}{\sigma^2 W}, \quad (5)$$

where $\mathbf{f} \in \mathbb{C}^{N_{\text{BS}}}$ is the beamforming vector in the BS side and $\mathbf{w} \in \mathbb{C}^{N_{\text{UE}}}$ is the combining vector in the UE side, W is the system bandwidth, σ^2 is the noise power level which is normalized by the transmit power. Due to the noise dominant nature of highly directional mmWave transmission [2], we omit the interference effect of other BSs. We define the achievable rate per second, between BS_j and UE in location i as $R(j, i) = W \log(1 + \text{SNR}(j, i))$.

In order to find the available path clusters between the BS_j and the UE in location i , we define a set of path skeletons, $\text{PS}(j, i) = \{p_1, \dots, p_P\}$ with size P . Each path p is defined based on AoA ($\theta_{r,p}^{\text{UE}}, \phi_{r,p}^{\text{UE}}$), AoD ($\theta_{r,p}^{\text{BS}}, \phi_{r,p}^{\text{BS}}$) and the channel gain ($\tilde{g} = \sqrt{\text{PL}(d)}$). Due to the sparsity of the mmWave channels in angular domain, P is a small number. Moreover, path skeleton sets have a correlation in adjacent locations [14]. A path skeleton can be identified using an exhaustive search method [9] or the proposed method in [14]. An example of a path skeleton, $\text{PS} = \{p_1, p_2\}$, between a BS and a UE is illustrated in Fig. 1. For the sake of simplicity, one subpath of each path cluster is shown in this figure.

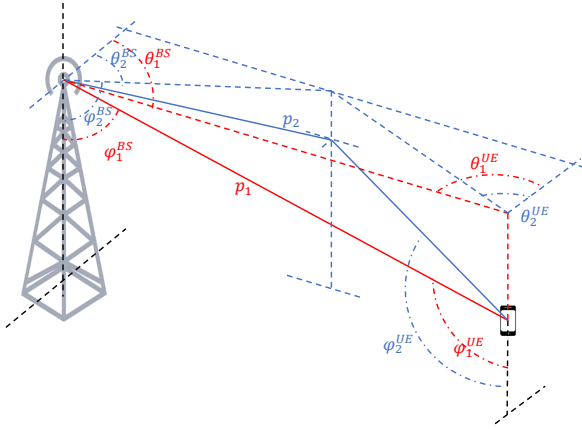


Fig. 1: An example of a path skeleton set contains a LoS path (p_1) and a NLoS path (p_2)

We define a zone based on a certain geographical area. We consider one agent for each zone that connects to all the BSs in its zone. Fig. 4 shows our simulation area and an example zone with five BSs. We consider the pedestrian and the vehicular mobility models, modeled through some trajectories. The different trajectories are shown in Fig. 4.

III. PROPOSED METHOD

During the mmWave handover process, there are multiple potential BSs to which the UE can connect. In mobile mmWave networks, the channel quality may drop quickly because of the mobility of the UE and temporary blockage by obstacles. Hence, re-execution of the beam-searching process to find a new serving BS may increase overhead and adversely impact on the UE throughput. In other words, beam searching with all the BSs in the UE's vicinity, increases the complexity of the handover process especially in moderate to high BS densities.

In order to address the aforementioned challenges, we propose to maintain an ordered list of backup BSs. In our proposed method, in case the link toward the serving BS dropped below a certain quality, a new link is established from the backup BS to the user with no need to search over all BS in the zone.

Our proposed handover mechanism consists of three components: pilot design and channel estimation, mobility prediction, and handover algorithm. We first design the pilot signals and then estimate the channel toward the serving BS using those pilots while assuming the mobility model of UE is available. Next, the handover execution decision is made based on the proposed handover algorithm. Our novel approach uses RL to select the backup channels and acquires the channel toward one non-serving BS at every coherent interval (CI). Using statistical data, we optimize this back-up inquiry process. In the following, we illustrate in detail these components.

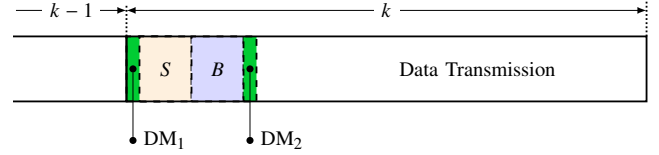


Fig. 2: Learning-based pilot design during CI k . Mini-slot S and mini-slot B are pilot transmission durations in order to estimate the channel toward serving BS and backup BS, respectively. DM_1 is the decision making phase regarding the choice of the backup BS. DM_2 is the decision making phase regarding the handover execution.

A. Channel Estimation

As shown in Fig. 2 for a CI k , our proposed pilot consists of a mini-slot S to acquire the channel toward the serving BS and mini-slot B for estimating the channel toward a backup BS. Each channel estimation mini-slot consists of P pilots, where P is the size of the path skeletons. We consider two decision making (DM) phases. In DM_1 , a backup BS for CI k will be determined based on the optimal policy of the RL algorithm and in DM_2 , the decision regarding the execution of the handover will be made. We define an acceptable handover threshold (T_{HO}) based on the user quality-of-service. In other words, during the DM_2 if the channel quality of the serving BS becomes lower than the predefined T_{HO} for a certain duration (which can be defined based on UE's quality-of-service), UE will switch to the backup BS. In the following, we will summarize our proposed efficient beamforming method, which we proposed in our recent work in [33].

In the channel estimation phase, we consider a path skeleton database in each BS that contains the path skeletons of different locations in the coverage area of every BS. However, having a path skeleton database entails two cost terms: query and maintenance. Query cost refers to the limited budget that BS can query a new path skeleton from the database and maintenance cost is the cost of building and keeping the database updated. First, we focus on the query cost and assume that an updated path skeleton database is available for all BSs. Then, we discuss the maintenance cost.

During the pilot transmission phase, the UE requests the path skeleton of its current location (x_i, y_i) from the serving BS $_j$. The pilot sequence is sent through the P paths of $PS(j, i)$ in order to estimate the channel between the UE and the BS. This estimation will then be used to design a precoding vector (\mathbf{f}) at the BS (from a given codebook \mathcal{F}) and a combining vector (\mathbf{w}) at the UE (from a given codebook \mathcal{W}) for the data transmission phase. Formally, we solve the following beamforming optimization problem:

$$\underset{\mathbf{f}, \mathbf{w}}{\text{maximize}} \quad |\mathbf{w}^H \mathbf{H} \mathbf{f}|^2 \quad (6a)$$

$$\text{subject to} \quad \mathbf{f} \in \mathcal{F}, \quad (6b)$$

$$\mathbf{w} \in \mathcal{W}. \quad (6c)$$

In an environment with a small number of scatters, the optimal beamforming and combining may adjust to the array response

of the strongest available path [2]. More details regarding the solution of (6) is provided in Appendix A.

Due to the correlation of the path skeletons in adjacent locations [33], there is no need to query a new path skeleton in every location of the UE. In other words, the BS can track the path skeleton changes and only ask a new beamforming solution when the current one is blocked or weakened by the obstacles. We consider the current path skeleton as the reference path skeleton $PS(j, 0)$ that is known to both the UE and the BS_j . In a new location (x_i, y_j) , the agent uses $PS(j, 0)$ to estimate $PS(j, i)$ and $\mathbf{H}(j, i)$. We define the distance between the reference path skeleton and estimated path skeleton as a metric to assess the validity of using the reference path skeleton in the new location (x_i, y_i) :

$$d(x_i, y_i; x_0, y_0) = \|PS(j, i) - PS(j, 0)\|_2. \quad (7)$$

Observations of [33] show that once the distance is sufficiently close (namely $d(x_i, y_i; x_0, y_0) \leq T_D$ for some small positive T_D), the UE can use $PS(j, 0)$ to estimate the channel $\mathbf{H}(j, i)$ in the new location. Otherwise, BS_j declares a significant change in the dominant paths. It then queries a new path skeleton and informs the UE. In this case, the reference path skeleton will be updated to the new path skeleton and BS_j tracks the validity of this new reference skeleton for beam-searching over time. We define T_D as the decision threshold that highly depends on the network topology. Smaller T_D results in frequent updates of the path skeletons and a higher overhead cost. Larger T_D reduces the network overhead but may result in sub-optimal selected beamforming and combining directions through the UE trajectory. In order to choose the optimal T_D for a limited query budget (U_{\max}), we run our algorithm for different mobility models and trajectories in the coverage area of all BSs. For instance, in the coverage area of BS_j , the optimal threshold $T_D^*(j)$ for pedestrian mobility model is the solution of the following optimization problem:

$$T_D^* = \underset{T_D > 0}{\operatorname{argmax}} \sum_{i \in [M]} \mathbb{E}[R(j, i)] \quad (8a)$$

$$\text{subject to } \Pr\{U > U_{\max}\} \leq \delta, \quad (8b)$$

where $R(j, i)$ is the rate between the UE in location i and BS_j , U is the number of times the PS renewed, and δ is a small given parameter. We have chosen $\delta = 0.2$ in our framework. In order to solve the optimization problem, we have used a well-known golden-section search method [34, Section 7.2] through a dataset of different pedestrian trajectories with length M . Note that if the estimated value of $\Pr\{U > U_{\max}\}$ is greater than δ , we assume the corresponding value of the objective function is $-\infty$. Note that these processes are done offline, so the complexity does not cause delay to the real time system.

The efficiency of our proposed beamforming method can be defined based on three parameters: computational and signaling complexity, throughput efficiency and energy consumption. In terms of throughput, our approach guarantees a close-to-optimal performance by updating the beamforming and combining vectors. Moreover, by sending pilots only over the path skeletons, our approach substantially reduces the beam searching overhead (the number of beams required to find

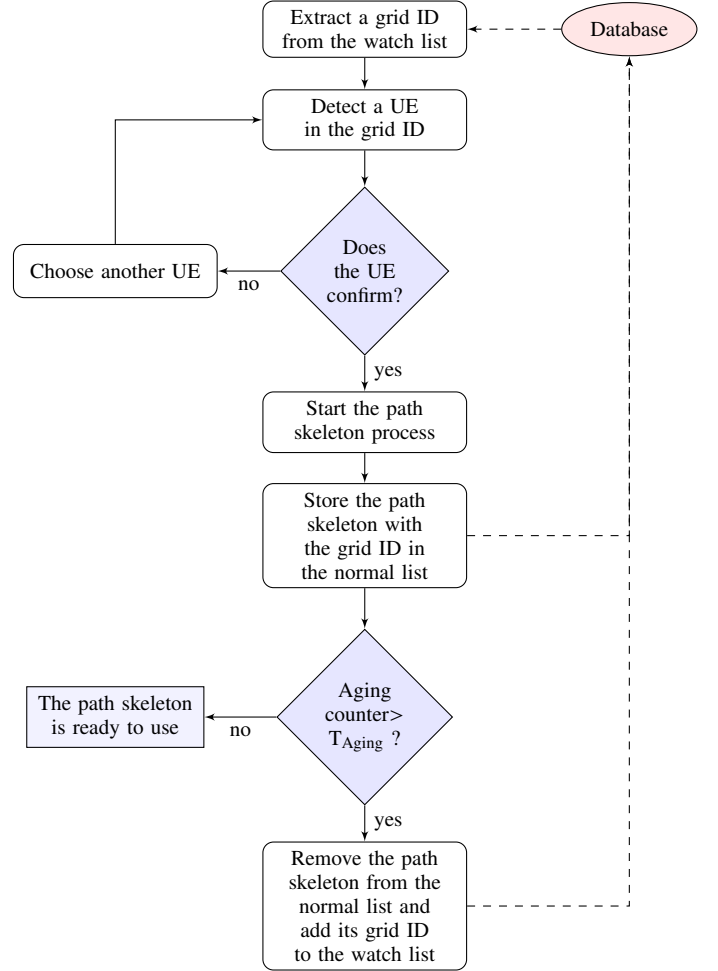


Fig. 3: The process of building and updating the database. First, a gridID is extracted from the watch list. If a detected UE in the grid ID approves the path skeleton finder request, the process starts and the skeleton set stores in the normal list with active aging counter. If the value of the aging counter exceeds the aging threshold, the skeleton set is removed from the normal list and its grid ID is added to the watch list. In this case, the algorithm returns to the skeleton finder loop [33].

the best alignment), making it efficient in terms of energy consumption, computational and signaling complexity.

Now, we present our approach regarding the building and maintaining the path skeleton database. In this case, we assume that every BS divides its coverage area to small grids and assigns a unique ID to them. The size of all the grids is equal and is chosen based on the network topology and balancing the complexity of building a database. Each grid is approximated to one point and one path skeleton is recorded for each grid ID in the database. In other words, only one path skeleton finding process (like the one in [14] or exhaustive beam-searching [9]) will run for each grid in order to build the path skeleton.

The path skeleton database has the normal list and the watch list that can be defined as the list of grid IDs with updated path skeletons and a list of grid IDs whose path skeletons are needed to be updated, respectively. As it is shown in Fig. 3, a BS sends the path skeleton finder request to the UEs in

every grid ID. It is important to note that a UE may refuse the request due to for example low battery level. If a UE accepts the request, the skeleton finder process will start and the skeleton is recorded in the normal list with a specific aging counter. If the aging counter of grid IDs in the normal list exceeds the predefined threshold (T_{Aging}), the BS will remove them from the normal list and adds them to the watch list. Fig. 3 illustrates this process.

T_{Aging} depends heavily on the network topology. In a crowded urban environment, the channel conditions will change rapidly so the database may need frequent updates. It means that T_{Aging} should be shorter for a highly dynamic environment compared to a stationary environment.

The overhead of the building and updating the database can be defined as the number of path skeleton finder requests that a UE will receive through its trajectory. In the crowded urban environment that the number of UEs is high, the database overhead is divided between all the users. Hence, the database overhead is almost negligible. More details of the proposed algorithm and performance evaluations are available in our recent work in [33].

Notice that there are two overhead terms involved with path skeleton. A) path skeleton database, which maintains the most updated path skeletons and B) beam-searching over an existing path skeleton. Upon handover, we only have the overhead B, whose complexity scales with the path sets in the skeleton. This cardinality is very small due to the sparse scattering nature of a mmWave channel. The main overhead comes from A, which we continuously run in background, even when no handover is requested. In particular, the BS sends the path skeleton finder request to the UEs in different grids. If the UE accepts this request, this process will be started. In the case that a grid does not have any UEs or all the UEs in that grid reject the path skeleton finder request, BS will start the path skeleton building process when a UE in that grid aims to establish a new connection or a handover. In other words, in the worst case, our method works like the existing methods for beam-searching based on path skeleton. However, such extreme case may rarely happen in a realistic urban environment. For example, assume that there exists U UEs in each grid ID at each time slot and each one of them accepts the path skeleton building request with probability p , independent to the other UEs¹. Hence, the probability that no UE accepts the request during T_{Aging} slots decreases with U and T_{Aging} , i.e., $(1 - p)^{UT_{\text{Aging}}}$.

B. Mobility Prediction

The mobility behavior and localization of the UEs are the important challenges in communication networks due to the key applications in handover and resource management [35]. An accurate prediction of the mobility pattern in dense mobile networks reduces the signaling overhead during the handover process [36], [37] and provides better quality-of-service and continuous connections.

As it is shown in [38] the mobility behavior of UEs in mmWave networks is predictable with good performance.

Most of the mobility patterns like pedestrians or vehicles are destination or direction oriented. The different mobility prediction schemes existing in the literature use Markov chain, hidden Markov model, artificial neural networks, Bayesian network and data mining (for more details see [38]). The outputs of these prediction methods are the UE's moving direction, transition probability to the next location, the future location and the trajectory [38], [39]. Studies in [23], [40] show that due to the use of the massive antenna arrays and the presence of the multi-path channel in mmWave networks, the performance of UE's localization is sufficiently high in both uplink and downlink communication. In this work, we assume that the mobility prediction information includes the UE's current location and its trajectory are available. The agent provides the mobility information to all BSs in its zone.

C. Handover Algorithm

As mentioned in the previous subsection, the mobility prediction information, including UE's trajectory with length M and its current location $i \in [M]$, is the input to our proposed handover algorithm. We assume one agent for a zone with N BSs where $j \in [N]$ is the index of BSs.

We quantize $\text{SNR}(j, i)$ to L levels. During the channel estimation in both mini-slots S and B , we only report the SNR level $\text{SNR}^{\ell, p^*}(j, i)$, $\ell \in [L]$, where p^* is the strongest path cluster over $\text{PS}(j, i)$, $p^* = \text{argmax}_p h_{r, p}$, $p \in \text{PS}(j, i)$. For the sake of notation simplicity, we drop the superscript of p^* and write $\text{SNR}^\ell(j, i)$. We define the handover threshold (T_{HO}) as the minimum acceptable SNR level. This parameter is determined based on the target quality-of-service level of the UE.

For the tagged UE, t_{Log} denotes the age of the current SNR log toward BS_j in term of the number of CIs. The initial value of the t_{Log} for all BS_j , $j \in [N]$ is equal to $t_{\text{Log}} = +\infty$. Once $\text{SNR}^\ell(j, i)$ is obtained for any $i \in [M]$, $t_{\text{Log}}(\text{BS}_j)$ is set to zero. At the end of each CI k , $k \in \{1, 2, \dots\}$, $t_{\text{Log}}(\text{BS}_j)$, $\forall j \in [N]$ is increased by 1 to indicate the age of the current log.

As it is illustrated in Algorithm 1, in location i and CI k channel estimation toward the serving BS (BS_S^k) and backup BS (BS_B^k) starts during the mini-slot S and mini-slot B , respectively. If the SNR level of BS_S^k remains above T_{HO} , the serving BS in the next CI will not be changed; otherwise, the handover decision will be made during DM_2 . If the SNR level of BS_S^k drops lower than T_{HO} , for a certain time interval, the handover will be triggered. Then, a BS with an acceptable SNR (larger than T_{HO}) and a minimum amount of t_{Log} (the most recent SNR updated) will be selected as the main candidate for the handover.

Illustrative Example 1: Consider a zone with four BSs. The SNR is quantized to two levels $\{\ell_1, \ell_2\}$ and T_{HO} is equal to ℓ_1 . Assume that in CI 3, the $\text{BS}_S^3 = \text{BS}_1$ and $\text{BS}_B^3 = \text{BS}_4$. The channel estimation will be done during mini-slots S and B and the SNR level and t_{Log} of BS_1 and BS_4 will be updated. Now in DM_2 the decision regarding the handover execution will be made. As it is shown in the following table, the SNR level of BS_1 and BS_4 are lower than T_{HO} , so the handover will run and the decision is the most recent updated BS with

¹This simple model, while not being realistic, gives the insights.

SNR level equal to ℓ_2 . In this case between BS₂ and BS₃, the BS₂ is selected because $t_{\text{Log}}(\text{BS}_2) < t_{\text{Log}}(\text{BS}_3)$. At the end of the CI 3, t_{Log} for all BS is increased by 1.

BS ID	BS ₁	BS ₂	BS ₃	BS ₄
SNR level	ℓ_1	ℓ_2	ℓ_2	ℓ_1
t_{Log}	0	1	2	0

The SNR log table will be updated in all the CIs and all UE's locations. During the DM₁ phase, the backup BS is selected based on the optimal policy of the RL algorithm, described in the next section. It worths to mention that if an appropriate backup BS is selected, the previous records in log table will not be checked. Therefore, if the agent is trained well enough, the probability that a proper backup BS is selected is high.

IV. LEARNING FRAMEWORK

The performance of the proposed handover approach heavily depends on how to select a backup BS in various CIs. This selection depends on the predictions of the SNR values and blockage of the BSs in future CIs. Such predictions, however, require a very detailed modeling of formidable complexity due to dynamicity of the obstacles and the UE mobility in mmWave networks. To address this problem, we use the RL framework to optimize the list of the backup BSs in various CIs.

The RL problem consists of a set of environment states \mathcal{S} , a set of actions $\mathcal{A}(s)$, a set of rewards $\mathcal{R} \subset \mathbb{R}$, and transition probabilities that determine the next state based on the current state and action [41]. In our problem, the transition probabilities model the SNR variations due to the UE's mobility through its trajectory and obstacle topology. The agent is the decision maker (which can sit in the edge cloud) based on the policy. More details regarding RL components are reported in Appendix B.

As it is shown in Fig. 4, all the BSs in a zone are connected to the agent. We define states as tuple $s = (s^{(1)}, s^{(2)}, s^{(3)}) \in \mathcal{S}$ where $s^{(1)} \in [M]$ is the current location of the UE through the trajectory with length M , $s^{(2)} \in [N]$ is the index of the serving BSs in the zone and $s^{(3)} \in [L]$ is the quantized SNR levels. The agent's action, $a \in \mathcal{A} = [N]$, is choosing a BS in order to ping as the backup BS. The SNR of the backup channel is estimated in mini-time B .

We define the agent's instantaneous reward as UE's achieved rate at the end of the CI as

$$r(s_i) = R(i)$$

and agent's long-term reward is the UE's trajectory rate (R_{traj}) as

$$R_{\text{traj}} = \sum_{i=1}^M R(i). \quad (9)$$

Therefore, the aim of the RL algorithm is to find the optimal policy (π^*) that maximizes the total UE's achieved rate through its trajectory, i.e.,

$$\pi^* = \underset{\pi}{\operatorname{argmax}} \mathbf{E} [R_{\text{traj}}], \quad (10)$$

Algorithm 1 Handover.

Inputs: UE's mobility model including current location of the trajectory $i \in [M]$, number of BSs in the UE's zone (N) and handover threshold (T_{HO}).

```

1: Initialization: For  $k = 1$  set  $\text{BS}_S^1 = \text{BS}_1$ 
2:  $t_{\text{Log}}(\text{BS}_j) = +\infty$ , for all  $j \in [N]$ 
3: for  $i = 1, \dots, M$  do
4:    $k \leftarrow$  current CI
5:   // During mini-time slot  $S$ 
6:   Estimate channel from  $\text{BS}_S^k$  toward location  $i$  and
7:   calculate the  $\text{SNR}(\text{BS}_S^k, i)$  level
8:   Set  $t_{\text{Log}}(\text{BS}_S^k) = 0$ 
9:   // During mini-time slot  $B$ 
10:  Choose  $\text{BS}_B^k = \text{BS}_j$ ,  $j \in [N]$  based on DM1
11:  Estimate channel from  $\text{BS}_B^k$  toward location  $i$  and
12:  calculate the  $\text{SNR}(\text{BS}_B^k, i)$  level
13:  Set  $t_{\text{Log}}(\text{BS}_B^k) = 0$ 
14:  if  $\text{SNR}^\ell(\text{BS}_S^k, i) > T_{\text{HO}}$  then
15:     $\text{BS}_S^{k+1} = \text{BS}_S^k$ 
16:  else
17:    // Perform handover
18:    if  $\text{SNR}^\ell(\text{BS}_B^k, i) > T_{\text{HO}}$  then
19:       $\text{BS}_S^{k+1} = \text{BS}_B^k$ 
20:    else
21:       $\text{BS}_S^{k+1} = \text{BS}_j$ , where
22:       $\hat{j} = \operatorname{argmin}_j t_{\text{Log}}(\text{BS}_j)$  s.t.  $\text{SNR}^\ell(j, i) > T_{\text{HO}}$ 
23:    end if
24:  end if
25:   $t_{\text{Log}}(\text{BS}_j) = t_{\text{Log}}(\text{BS}_j) + 1$ , for all  $j \in [N]$ 
26: end for
27: Outputs:  $\text{BS}_S$  and  $R_i$  for all  $i \in [M]$ 

```

where the expectation is with respect to the randomness in the channel gain (fading and blockage).

In our case π is a function from $\mathcal{S} \subseteq \mathcal{R}$ to $\mathcal{A} = [N]$, i.e.,

$$\pi : [M] \times [N] \times [L] \mapsto [N].$$

So, π is a 3-dimensional array which shows the best choice of backup BS for each state.

In order to find π^* , we use Q-learning algorithm, which enables learning with no prior knowledge of the environment and finds the optimal decision based on the interactions with the environment, using Algorithm 2 [41]. In Appendix C, we have provided more detailed information on the Q-learning and how it works.

V. SIMULATION RESULTS

In this section, we present the performance evaluation of our proposed method in compared to state-of-the-art benchmarks. We consider the downlink of mmWave network operating at 28 GHz in two parts. In the first part, we use the narrow band cluster 3D channel model with different BS densities and in the second part, we use ray tracing tool to simulate a more realistic blockage and mmWave channel model. In all simulations, we fix the UE's trajectory. We consider a zone of $100 \times 100 m^2$ area. The topology and the trajectories are

Algorithm 2 Q-Learning in ϵ -greedy policy in one episode [41]

- 1: Initialization: An initial value $Q(s, a) \forall s \in \mathcal{S} = [M] \times [N] \times [L], \forall a \in \mathcal{A}(s) = [N]$
 - 2: **for** $i \in [M]$ **do**
 - 3: Observe s_i
 - 4: Take a random variable τ uniformly from $[0,1]$
 - 5: **if** $\tau \leq \epsilon$ **then**
 - 6: Take a random action a_i uniformly from set $\mathcal{A}(s)$
 - 7: **else**
 - 8: Take action $a_i = \operatorname{argmax}_{a \in \mathcal{A}(s)} Q^*(s, a)$
 - 9: **end if**
 - 10: Observe s_{i+1} and $r(s_i)$
 - 11: Update the action-value function as:
 - 12: $Q(s_i, a_i) \leftarrow Q(s_i, a_i) + \alpha [r(s_i) + \gamma \max_{a \in \mathcal{A}(s_{i+1})} Q(s_{i+1}, a) - Q(s_i, a_i)]$
 - 13: **end for**
-

shown in Fig. 4. The simulation parameters are listed in Table II.

We compare the performance of our proposed handover method with two baselines: *multi-connectivity* handover [26] and *SMART* handover [20]. In the *multi-connectivity* handover baseline, the UE constantly checks the SNR of all the BS links in the zone and when experiences the blockage of the serving BS link, selects a BS with the highest quality. Although this baseline may provide an upper bound for the quality of the service [26], it suffers from the high computational complexity. The *SMART* baseline is based on an RL handoff policy which reduces the number of the handovers while keeps the UE's quality-of-service. In this baseline, the BS selection algorithm is based on Upper Confidence Bound (UCB) algorithm [42] which has low complexity and achieves the optimal solution asymptotically. The UCB algorithm estimates $\mathbf{E}[r(s, a)]$ by uniformly averaging the previously received rewards in state s and action a . Then, it solves a set of equations which their solutions asymptotically converge to the solution of the Bellman equation. In *SMART* algorithm the reward is the rate of the UEs and the set of equations are obtained by adding a term to the reward [20].

To evaluate the performance of our proposed beamforming method, we use the approach of [15] as a baseline. In this baseline, the path skeleton sets are updated based on a fixed Euclidean distance (ED). However, in our beamforming method the optimal path skeleton distance threshold (T_D) is found based on Equation (8).

A. Narrow Band Cluster Channel Model

In this model, we generate the mmWave links as described in Section II. We consider a UE with a trajectory of 100 m and two mobility models in our numerical studies: pedestrian and vehicle, where we assumed a UE speed of 5 km/h and 36 km/h, respectively. Due to the similarity of the results, we only report the pedestrian mobility model in the following.

We use 10^5 different channel realizations as the input of the RL algorithm. During the learning phase, we run our

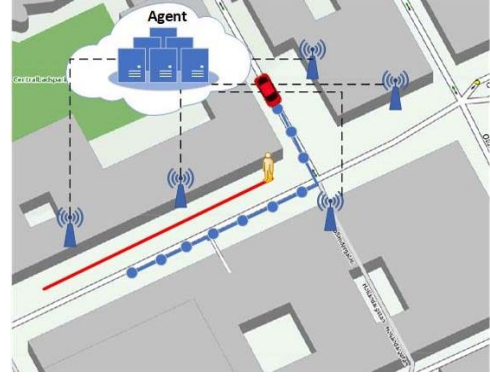


Fig. 4: Simulation area. The red line shows the trajectory of a pedestrian. The blue line shows a vehicular trajectory whose location indexes are denoted by circles. The dash lines illustrate that all of the BSs are connected to the agent.

Table II: Simulation parameters.

Parameters	Values in Simulations
BS transmit power	30 dBm
σ^2	-174 dBm/Hz
W	500 MHz
N_{BS}	8×8
N_{UE}	4×4
\hat{n}_{LoS}	3
\hat{n}_{NLoS}	4
Ray tracing parameters	
BS height	6 m
Brick penetration loss [43]	28.3 dB
Glass penetration loss [43]	3.9 dB
learning parameters	
α	0.1
γ	0.99
ϵ	0.01

algorithm in order to reach the optimal policy that in this case, is the selecting optimal backup BS in different states². The handover threshold is $T_{HO} = 40$ dB. Based on the speed of the pedestrian, we define location indexes in every 2 m (50 location indexes through the trajectory). We fix the maximum number of path skeleton updated (U_{max}) to 10. We choose the distance between two consecutive updates in the ED approach equals to 10 m to keep the same U_{max} as our approach. We study two different scenarios with different BS densities as follows:

1) *First Scenario (sparse mmWave network)*: In the first scenario, we consider a BS density of $\rho = 5 \times 10^{-4}/m^2$, which corresponds to the average of one BS in every $50 m^2$. After finding the optimal policy, we run our proposed algorithm over 10^4 different channel realizations. Fig. 5 compares the performance of our approach to the baselines. In *our approach*, we use our proposed beamforming method and handover algorithm. In *our approach-ED*, we use the ED approach to trigger beamforming in our handover algorithm. In *multi-connectivity* and *SMART* baselines, we apply our skeleton-based beamforming method while using their handover algo-

²In our case, in order to converge to the optimal solution, we run our algorithm 10^6 times. The running time by using a standard desktop computer is around 6 hours.

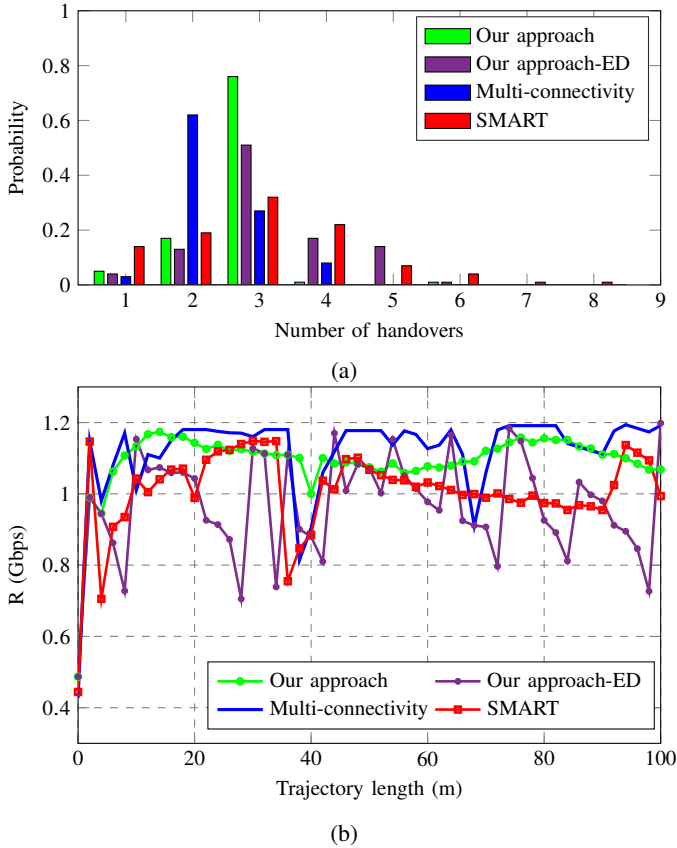


Fig. 5: Handover performance of our approach compared to baselines in a sparse mmWave network.

gorithms. In particular, Fig. 5a shows the number of handovers when the UE moves along the trajectory, and Fig. 5b shows the average $R(i)$, $i \in [100]$. The average trajectory rate, R_{traj} , in this scenario is shown in Table III. It can be seen from the figure that our proposed learning-based handover provides almost a same rate in all locations of the trajectory with a small number of the handovers. Even in the case of handover, our approach can maintain an almost constant rate for the UE, making it suitable for services with high reliability requirements. Moreover, based on Table III, our approach provides high trajectory rate by considering the long term effects of the handovers. The baselines, however, suffer from either high number of handovers or high fluctuations on R_i . In *our approach-ED*, non-optimal path skeleton updating causes higher rate fluctuations and higher number of handover needed compared to *our approach*. In the case of *Multi-connectivity* baseline, the additional connection-probe procedure increases the complexity of the method from the UE's perspective.

2) *Second Scenario (dense mmWave network)*: In the second scenario, the density of the BSs is $\rho = 10^{-3}/m^2$ which corresponds to the average of one BS in every $30 m^2$. Fig. 6a illustrates the number of the handovers, and Fig. 6b shows the average $R(i)$, $i \in [100]$. It is evident that our learning-based handover method due to having less rate fluctuations along the trajectory is more reliable handover method specially when a high quality-of-service is needed. Furthermore, our method

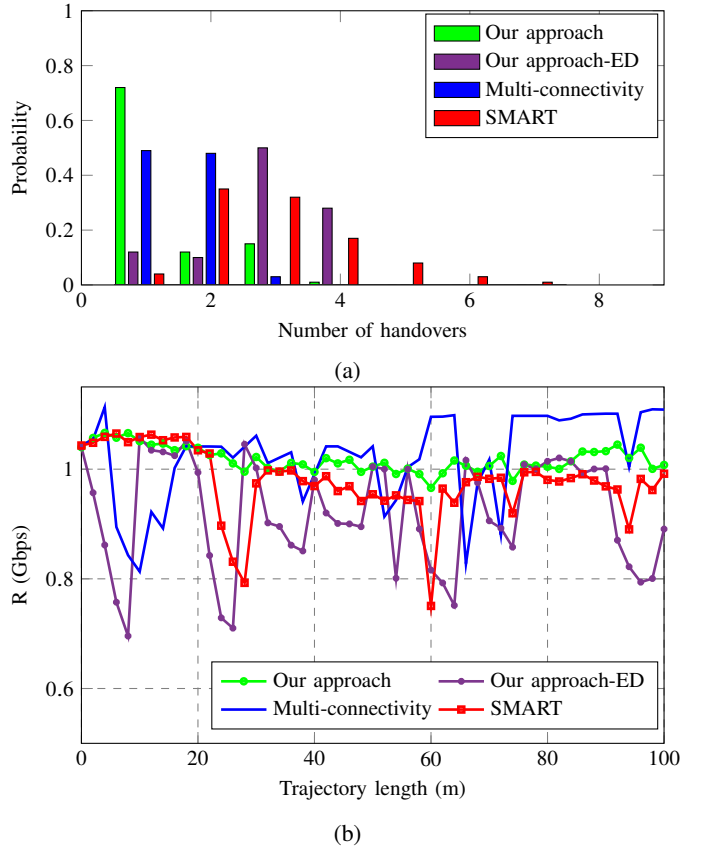


Fig. 6: Handover performance of our approach compared to baselines in a dense mmWave network.

Table III: Average trajectory rate, R_{traj} , (Gbps).

Methods	Sparse scenario	Dense scenario
Our approach	55.65	51.90
Our approach-ED	52.13	50.03
Multi-connectivity	57.08	52.17
SMART	51.39	49.8062

keeps the number of handover needed small while providing comparable $R(i)$ and R_{traj} (as it is shown in Table III) in comparison to other two baselines and *our approach-ED*.

B. Ray Tracing

We have also used ray tracing to model and evaluate the performance of our approach in a more realistic environment. In this part, we use our beamforming method as described in Section III-A and evaluate the performance of our proposed handover algorithm. For the network topology, we extracted the real building map of the central part of Stockholm city from *open street map* data as the input of the ray tracing tool [44]. Then, we randomly assigned brick or glass materials to the buildings as the permanent obstacles. We also added some temporary random obstacles with height 1.5 m to model human bodies and some temporary random obstacles with width 4 m and heights 1 m and 3 m to model various vehicles with different heights. The number, the position and the material loss of the temporary obstacles were chosen

randomly in each realization of the channel. The simulation area is illustrated in Fig. 4. UEs are moving along the real streets as extracted from *open street map* data. We consider the UE's trajectory with length 100 m and the vehicle mobility model. We consider the location indexes every 10 m (11 location indexes through the trajectory) as it is shown with the blue line in Fig. 4. The density of the BSs is $\rho = 5 \times 10^{-4}/m^2$. The handover threshold is $T_{HO} = 0$ dB.

We run the ray tracing simulator for all the BSs for different topologies. We considered each topology with different distribution and density of the temporary obstacles.

As it can be seen in Fig. 7, our proposed solution needs less number of the handovers while keeps the rate in each location almost consistent in comparison to other two baselines. Moreover, our approach by selecting the optimal actions in each state provides a near maximum long term reward (R_{traj}) as it is shown in Table IV.

VI. CONCLUSIONS

In this paper, we jointly considered the beamforming and handover challenges in mobile mmWave networks. We proposed an efficient beamforming method which leverages the sparsity and the spatial correlation of path skeletons in the channel estimation phase. We designed a handover algorithm based on a pilot structure that consists of an extra mini-slot regarding channel estimation toward backup BS. We used reinforcement learning algorithm as a decision maker regarding the choice of the backup BS in all locations of the UE's trajectory. Our proposed algorithm triggers a handover to a backup channel when the link quality drops below a predefined threshold. We evaluated the performance of our method based on the narrow band cluster channel model and ray tracing. The results showed that our approach provides a reliable connection with the consistent rate through the UE's trajectory.

For future work, we plan to consider the load balancing and resource management in our joint beamforming and handover approach. Moreover, we plan to work on an accurate mobility prediction scheme using the tracking and localization capabilities of the mmWave networks.

APPENDIX A

In order to solve (6), we define matrices $\mathbf{G} \in \mathbb{C}^{|\mathcal{W}| \times |\mathcal{F}|}$, $\mathbf{W} \in \mathbb{C}^{d_w \times |\mathcal{W}|}$, $\mathbf{F} \in \mathbb{C}^{d_f \times |\mathcal{F}|}$ as following

$$\begin{aligned} \mathbf{W} &:= [\mathbf{w}_1 \ \mathbf{w}_2 \ \dots \ \mathbf{w}_{|\mathcal{W}|}], \\ \mathbf{F} &:= [\mathbf{f}_1 \ \mathbf{f}_2 \ \dots \ \mathbf{f}_{|\mathcal{F}|}], \\ \mathbf{G} &:= \mathbf{W}^H \mathbf{H} \mathbf{F}, \end{aligned}$$

where d_w and d_f are the dimension of codewords in \mathcal{W} and \mathcal{F} , respectively; $\mathbf{w}_a \in \mathcal{W}$ and $\mathbf{f}_b \in \mathcal{F}$ are the codewords, so \mathbf{W} and \mathbf{F} are made by concatenating all codewords. It can be obtained that for $\mathbf{w}_a \in \mathcal{W}$ and $\mathbf{f}_b \in \mathcal{F}$, $g_{a,b} = \mathbf{w}_a^H \mathbf{H} \mathbf{f}_b$. Hence, in order to find the solution of (6), one only needs to find a^* , b^* such that $|g_{a^*,b^*}|^2 \geq |g_{a,b}|^2$ for all $a \in [|\mathcal{W}|]$, $b \in [|\mathcal{F}|]$. As a result, \mathbf{w}_{a^*} , \mathbf{f}_{b^*} is the optimal solution of (6).

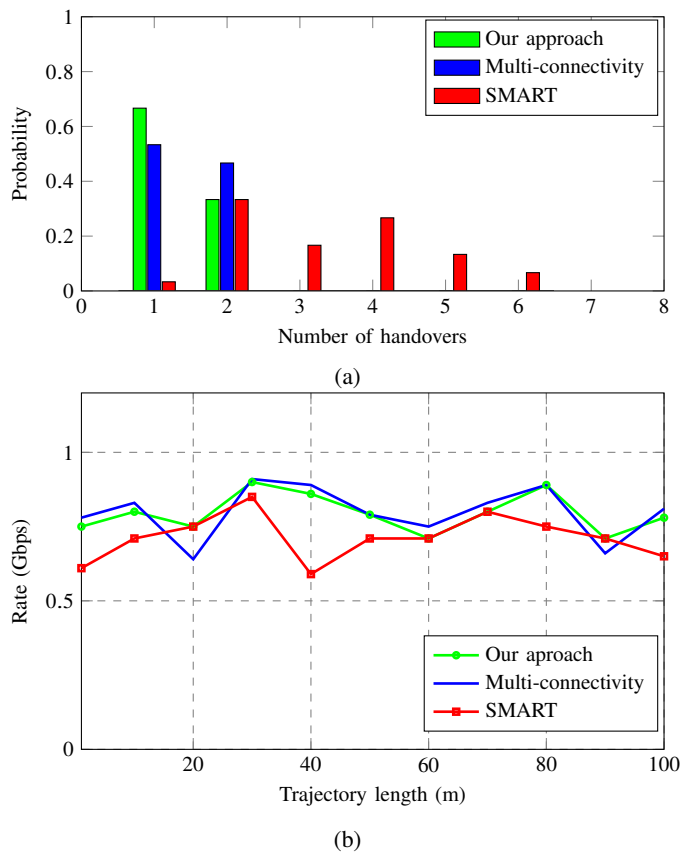


Fig. 7: Handover performance of our approach compared to baselines for simulated data. Topology is given by Fig. 4.

Table IV: Average trajectory rate, R_{traj} , (Gbps).

Methods	Ray tracing
Our approach	8.74
Multi-connectivity	8.78
SMART	7.87

APPENDIX B REINFORCEMENT LEARNING

In this part, we introduce the reinforcement learning (RL) model as a decision making tool. At each step k , the agent makes a decision regarding a new action based on the immediate received reward of its action in the previous step. The agent interacts with the environment in order to maximize the reward while exploring the environment. The main goal of the agent in RL is learning the optimal policy π^* in order to maximize its long-term reward. In particular, the agent maximizes the expected discounted reward and finds the optimal policy as [41]:

$$\pi^* = \underset{\pi}{\operatorname{argmax}} \mathbf{E} \left[\sum_{k=0}^{\infty} \gamma^k r(S_k, A_k) \middle| S_0 = s \right], \quad (11)$$

where $r(S_k, A_k)$ is the reward that the agent receives in time k and $\gamma \in [0, 1]$ is the discount factor. The expectation is with respect to the randomness of the states.

In episodic learning, the interactions between the agent and the environment is divided into subsequences of consecutive

steps which are called episodes [41]. Each episode has a limited number of steps. In our scenario, each running of a fixed trajectory with a random distribution of the temporary obstacles is considered as an episode with length M where M is the length of the trajectory.

APPENDIX C Q-LEARNING

The optimal action-value function $Q^*(s, a)$ is defined as:

$$Q^*(s, a) = \max_{\pi} \mathbf{E} \left[\sum_{k=1}^{\infty} \gamma^k r(S_k, A_k) \middle| S_0 = s, A_0 = a \right] + \mathbf{E}[r(s, a)] \quad (12)$$

$$= \max_{a \in \mathcal{A}(s)} \mathbf{E}[Q^*(S_1, a) | S_0 = s, A_0 = a] + \mathbf{E}[r(s, a)], \quad (13)$$

where the proof of the last equality can be found in [41, Section 3.6]. The optimal policy π^* of the agent is

$$\pi^*(s) = \operatorname{argmax}_{a \in \mathcal{A}(s)} Q^*(s, a), \quad \forall s \in \mathcal{S}. \quad (14)$$

Based on Q-learning in ϵ -greedy policy, agent takes action $a_i = \operatorname{argmax}_{a \in \mathcal{A}(s)} Q_i(s_i, a)$ in state $s_i \in \mathcal{S}$ with probability $1 - \epsilon$ or a random action with probability ϵ where $\epsilon \in [0, 1]$ and $Q_i(s, a)$ is the estimation of the Q function in step i . In next state $s_{i+1} \in \mathcal{S}$, the agent observes the reward and updates the action-value function $Q_{i+1}(s, a)$ [41].

REFERENCES

- [1] T. S. Rappaport, F. Gutierrez, E. Ben-Dor, J. N. Murdock, Y. Qiao, and J. I. Tamir, "Broadband millimeter-wave propagation measurements and models using adaptive-beam antennas for outdoor urban cellular communications," *IEEE Transactions on Antennas and Propagation*, vol. 61, no. 4, pp. 1850–1859, Apr. 2013.
- [2] M. R. Akdeniz, Y. Liu, M. K. Samimi, S. Sun, S. Rangan, T. S. Rappaport, and E. Erkip, "Millimeter wave channel modeling and cellular capacity evaluation," *IEEE Journal on Selected Areas in Communications*, vol. 32, no. 6, pp. 1164–1179, Jun. 2014.
- [3] S. Kutty and D. Sen, "Beamforming for millimeter wave communications: An inclusive survey," *IEEE Communications Surveys & Tutorials*, vol. 18, no. 2, pp. 949–973, 2nd Quart, 2016.
- [4] H. Shokri-Ghadikolaei, C. Fischione, G. Fodor, P. Popovski, and M. Zorzi, "Millimeter wave cellular networks: A MAC layer perspective," *IEEE Transactions on Communications*, vol. 63, no. 10, pp. 3437–3458, Oct. 2015.
- [5] R. Baldemair, T. Irnich, K. Balachandran, E. Dahlman, G. Mildh, Y. Selen, S. Parkvall, M. Meyer, and A. Osseiran, "Ultra-dense networks in millimeter-wave frequencies," *IEEE Communications Magazine*, vol. 53, no. 1, pp. 202–208, Jan. 2015.
- [6] T. S. Rappaport, S. Sun, R. Mayzus, H. Zhao, Y. Azar, K. Wang, G. N. Wong, J. K. Schulz, M. Samimi, and F. Gutierrez Jr, "Millimeter wave mobile communications for 5G cellular: It will work!" *IEEE Access*, vol. 1, no. 1, pp. 335–349, May 2013.
- [7] B. Yang, X. Yang, X. Ge, and Q. Li, "Coverage and handover analysis of ultra-dense millimeter-wave networks with control and user plane separation architecture," *IEEE Access*, vol. 6, pp. 54 739–54 750, 2018.
- [8] "IEEE 802.15.3c Part 15.3: Wireless medium access control (MAC) and physical layer (PHY) specifications for high rate wireless personal area networks (WPANs) amendment 2: Millimeter-wave based alternative physical layer extension," Oct. 2009.
- [9] "IEEE 802.11ad. Part 11: Wireless LAN medium access control MAC and physical layer PHY specifications - amendment 3: Enhancements for very high throughput in the 60 GHz band," Dec. 2012.
- [10] R. W. Heath, N. Gonzalez-Prelcic, S. Rangan, W. Roh, and A. M. Sayeed, "An overview of signal processing techniques for millimeter wave MIMO systems," *IEEE Journal of Selected Topics in Signal Processing*, vol. 10, no. 3, pp. 436–453, Apr. 2016.
- [11] H. Ghauch, T. Kim, M. Bengtsson, and M. Skoglund, "Subspace estimation and decomposition for large millimeter-wave MIMO systems," *IEEE Journal of Selected Topics in Signal Processing*, vol. 10, no. 3, pp. 528–542, Apr. 2016.
- [12] Z. Marzi, D. Ramasamy, and U. Madhoo, "Compressive channel estimation and tracking for large arrays in mm-wave picocells," *IEEE Journal of Selected Topics in Signal Processing*, vol. 10, no. 3, pp. 514–527, Apr. 2016.
- [13] H. Hassanieh, O. Abari, M. Rodriguez, M. Abdelghany, D. Katabi, and P. Indyk, "Fast millimeter wave beam alignment," in *Proc. the Conference of the ACM Special Interest Group on Data Communication (ACM SIGCOM)*, 2018, pp. 432–445.
- [14] S. Sur, X. Zhang, P. Ramanathan, and R. Chandra, "Beamspy: Enabling robust 60 GHz links under blockage," in *Proc. 13th USENIX Symposium on Networked Systems Design and Implementation (USENIX NSDI)*, 2016, pp. 193–206.
- [15] A. Zhou, X. Zhang, and H. Ma, "Beam-forecast: Facilitating mobile 60 GHz networks via model-driven beam steering," in *Proc. IEEE Conference on Computer Communications (INFOCOM)*, 2017, pp. 1–9.
- [16] M. Mezzavilla, S. Goyal, S. Panwar, S. Rangan, and M. Zorzi, "An MDP model for optimal handover decisions in mmwave cellular networks," in *2016 European Conference on Networks and Communications (EuCNC)*, Jun. 2016, pp. 100–105.
- [17] Y. Sun, G. Feng, L. Zhang, P. V. Klaine, M. A. Iinran, and Y. Liang, "Distributed learning based handoff mechanism for radio access network slicing with data sharing," in *IEEE International Conference on Communications (ICC)*, May 2019, pp. 1–6.
- [18] E. Stevens-Navarro, Y. Lin, and V. W. Wong, "An MDP-based vertical handoff decision algorithm for heterogeneous wireless networks," *IEEE Transactions on Vehicular Technology*, vol. 57, no. 2, pp. 1243–1254, Mar. 2008.
- [19] S. Zang, W. Bao, P. L. Yeoh, B. Vucetic, and Y. Li, "Managing vertical handovers in millimeter wave heterogeneous networks," *IEEE Transactions on Communications*, vol. 67, no. 2, pp. 1629–1644, Feb. 2019.
- [20] Y. Sun, G. Feng, S. Qin, Y. Liang, and T. P. Yum, "The SMART handoff policy for millimeter wave heterogeneous cellular networks," *IEEE Transactions on Mobile Computing*, vol. 17, no. 6, pp. 1456–1468, Jun. 2018.
- [21] Y. Koda, K. Yamamoto, T. Nishio, and M. Morikura, "Reinforcement learning based predictive handover for pedestrian-aware mmwave networks," in *IEEE Conference on Computer Communications Workshops (INFOCOM WKSHPS)*. IEEE, 2018, pp. 692–697.
- [22] Y. Koda, K. Nakashima, K. Yamamoto, T. Nishio, and M. Morikura, "Handover management for mmwave networks with proactive performance prediction using camera images and deep reinforcement learning," *IEEE Transactions on Cognitive Communications and Networking*, vol. 6, no. 2, pp. 802–816, Jun. 2020.
- [23] C. Fiandrino, H. Assasa, P. Casari, and J. Widmer, "Scaling millimeter-wave networks to dense deployments and dynamic environments," *Proceedings of the IEEE*, vol. 107, no. 4, pp. 732–745, Apr. 2019.
- [24] S. Sur, I. Pefkianakis, X. Zhang, and K.-H. Kim, "Towards scalable and ubiquitous millimeter-wave wireless networks," in *Proceedings of the 24th Annual International Conference on Mobile Computing and Networking*. ACM, 2018, pp. 257–271.
- [25] R. Parada and M. Zorzi, "Context-aware handover in mmwave 5G using UE's direction of pass," in *24th European Wireless Conference*, 2018, pp. 1–6.
- [26] V. Petrov, D. Solomitckii, A. Samuylov, M. A. Lema, M. Gapeyenko, D. Moltchanov, S. Andreev, V. Naumov, K. Samouylov, M. Dohler, and Y. Koucheryavy, "Dynamic multi-connectivity performance in ultra-dense urban mmwave deployments," *IEEE Journal on Selected Areas in Communications*, vol. 35, no. 9, pp. 2038–2055, Sep. 2017.
- [27] M. Giordani, M. Mezzavilla, S. Rangan, and M. Zorzi, "An efficient uplink multi-connectivity scheme for 5G millimeter-wave control plane applications," *IEEE Transactions on Wireless Communications*, vol. 17, no. 10, pp. 6806–6821, Oct. 2018.
- [28] C. Tatino, I. Malanchini, N. Pappas, and D. Yuan, "Maximum throughput scheduling for multi-connectivity in millimeter-wave networks," in *16th International Symposium on Modeling and Optimization in Mobile, Ad Hoc, and Wireless Networks (WiOpt)*, May 2018, pp. 1–6.
- [29] M. Gapeyenko, V. Petrov, D. Moltchanov, M. R. Akdeniz, S. Andreev, N. Himayat, and Y. Koucheryavy, "On the degree of multi-connectivity in 5G millimeter-wave cellular urban deployments," *IEEE Transactions on Vehicular Technology*, vol. 68, no. 2, pp. 1973–1978, Feb. 2019.
- [30] I. A. Hemadeh, K. Satyanarayana, M. El-Hajjar, and L. Hanzo, "Millimeter-wave communications: Physical channel models, design

- considerations, antenna constructions, and link-budget,” *IEEE Communications Surveys & Tutorials*, vol. 20, no. 2, pp. 870–913, 2017.
- [31] M. K. Samimi, T. S. Rappaport, and G. R. MacCartney, “Probabilistic omnidirectional path loss models for millimeter-wave outdoor communications,” *IEEE Wireless Communications Letters*, vol. 4, no. 4, pp. 357–360, 2015.
- [32] T. S. Rappaport, G. R. MacCartney, M. K. Samimi, and S. Sun, “Wide-band millimeter-wave propagation measurements and channel models for future wireless communication system design,” *IEEE Transactions on Communications*, vol. 63, no. 9, pp. 3029–3056, 2015.
- [33] S. Khosravi, H. S. Ghadikolaei, and M. Petrova, “Efficient beamforming for mobile mmWave networks,” 2019. [Online]. Available: <https://arxiv.org/abs/1912.12118v1>.
- [34] E. Chong and S. Zak, *An Introduction to Optimization*, ser. Wiley Series in Discrete Mathematics and Optimization. Wiley, 2013.
- [35] Wee-Seng Soh and H. S. Kim, “QoS provisioning in cellular networks based on mobility prediction techniques,” *IEEE Communications Magazine*, vol. 41, no. 1, pp. 86–92, Jan. 2003.
- [36] A. N. Khan and S. X. Jun, “A new handoff ordering and reduction scheme based on road topology information,” in *International Conference on Wireless Communications, Networking and Mobile Computing*, Sep. 2006, pp. 1–4.
- [37] A. Mohamed, O. Onireti, S. A. Hoseinitabatabaei, M. Imran, A. Imran, and R. Tafazolli, “Mobility prediction for handover management in cellular networks with control/data separation,” in *IEEE International Conference on Communications (ICC)*, Jun. 2015, pp. 3939–3944.
- [38] H. Zhang and L. Dai, “Mobility prediction: A survey on state-of-the-art schemes and future applications,” *IEEE Access*, vol. 7, pp. 802–822, 2019.
- [39] R. Wu, G. Luo, J. Shao, L. Tian, and C. Peng, “Location prediction on trajectory data: A review,” *Big Data Mining and Analytics*, vol. 1, no. 2, pp. 108–127, Jun. 2018.
- [40] Z. Abu-Shaban, X. Zhou, T. Abhayapala, G. Seco-Granados, and H. Wymeersch, “Performance of location and orientation estimation in 5G mmwave systems: Uplink vs downlink,” in *IEEE Wireless Communications and Networking Conference (WCNC)*, Apr. 2018, pp. 1–6.
- [41] R. Sutton and A. Barto, *Reinforcement Learning: An Introduction*, ser. Adaptive Computation and Machine Learning series. MIT Press, 2018.
- [42] P. Auer, N. Cesa-Bianchi, and P. Fischer, “Finite-time analysis of the multiarmed bandit problem,” *Machine learning*, vol. 47, no. 2-3, pp. 235–256, 2002.
- [43] H. Zhao, R. Mayzus, S. Sun, M. Samimi, J. K. Schulz, Y. Azar, K. Wang, G. N. Wong, F. Gutierrez, and T. S. Rappaport, “28 GHz millimeter wave cellular communication measurements for reflection and penetration loss in and around buildings in New York City,” in *Pro. IEEE International Conference on Communications (ICC)*, 2013, pp. 5163–5167.
- [44] L. Simic, J. Riihijärvi, A. Venkatesh, and P. Mahoonen, “Demo abstract: An open source toolchain for planning and visualizing highly directional mm-wave cellular networks in the 5G era,” in *IEEE Conference on Computer Communications Workshops (INFOCOM WKSHPS)*, 2017, pp. 966–967.